Available online at www.sciencedirect.com
ScienceDirect
Journal of Sound and Vibration 311 (2008) 314–327
JOURNAL OF SOUND AND VIBRATION
www.elsevier.com/locate/jsvi

An experimental investigation into the use of scaling laws for predicting vibration responses of rectangular thin plates

Pairod Singhatanadgid*, Anawat Na Songkhla

Department of Mechanical Engineering, Faculty of Engineering, Chulalongkorn University, Bangkok 10330, Thailand

Received 4 January 2007; received in revised form 5 September 2007; accepted 11 September 2007
Available online 22 October 2007

Abstract

A scaling law for the vibration response of rectangular plates along with a similarity requirement was derived and validated with the experimental results in this study. The scaling law was derived from the governing equation of the problem and was found to be exact after verifying with a closed-form solution. An experimental investigation was conducted on several model and prototype specimens using an impact test method. The natural frequencies of the models were substituted into the scaling law to obtain the scaling natural frequencies of the prototypes, which were then compared with the measured natural frequencies. In the first part of the study, a total of nine aluminum rectangular plates with various boundary conditions were tested for natural frequencies to determine the size effect on the accuracy of the scaling law. From a total of 108 comparisons, the average percentage discrepancy of the scaling natural frequencies was 4.90% with a standard deviation of 6.45%. Therefore, the scaling law is satisfactorily accurate for a pair of models and prototypes of the same material but of different size. The other part of the study involved the investigation of the material's effect on the accuracy of the scaling law. The experimental results showed that, unlike theoretical verification, using model and prototype systems with different materials resulted in an erroneous scaling natural frequency. The predicted natural frequency was inaccurate in this case because the boundary conditions enforced by the supports on the models and prototypes of different materials were significantly different. Consequently, the similarity requirement between the model and prototype is violated in the case of this study. With an additional experiment, the scaling law was found to be practically accurate for model–prototype pairs of different materials if their similitude requirements were fulfilled. The possible sources of discrepancy of the scaling natural frequency include uncertainties of the experiment, incomplete similarity of plate configurations and non-identical boundary conditions between the prototype and its model.

1. Introduction

The similitude concept has been utilized in many engineering applications. The principle provides a powerful tool for engineers and scientists to replicate the behavior of the prototype using an appropriate scaled model. Similitude theory can be stated as [1]; "the sufficient and necessary condition of similitude between two systems is that the mathematical model of the one be related by a bi-unique transformation to that of the other." For a prototype of interest, a scaled replica can be built to duplicate the behavior of the

*Corresponding author. Tel.: +66 2 218 6595; fax: +66 2 252 2889.
E-mail address: Pairod.S@chula.ac.th (P. Singhatanadgid).

0022-460X/$ - see front matter © 2007 Elsevier Ltd. All rights reserved.
doi:10.1016/j.jsv.2007.09.006

full-scale system. The experimental results on the model can be utilized to predict the behavior of the prototype. The similitude concept is thus very useful, especially, for problems with either a complex domain or complicated boundary conditions for which numerical solutions are not sufficiently accurate, if possible. If the prototype is perfectly replicated, the experiment result on the model can be scaled to predict the behavior of the prototype with sufficient accuracy.

The similitude theory has been applied to many problems in the field of structural engineering, including vibration and buckling problems of plates. Simitses [2] applied similitude transformation to the bending, buckling, and vibration of laminated plates. The derived scaling laws were successfully employed to the problem with appropriate similarity requirements between model and prototype systems. Rezaeepazhand et al. [3] demonstrated a procedure for deriving a scaling law for the frequency response of laminated plates. Both Simitses and Rezaeepazhand derived scaling laws from the closed-form solutions of the problems. Alternatively, scaling laws can be derived directly from the governing equation of the problems. In Refs. [4–6], the authors derived the scaling laws for the vibration and buckling behavior of laminated rectangular plates. In those studies, similitude transformation was applied to the governing equations of the problems directly. Besides the scaling law, the similarity requirements were also obtained. An advantage of this approach is that a solution of the governing equations is not required. The obtained scaling laws were verified with the theoretical solution and found to be exact for complete similitude cases. Partial similitude cases were also investigated and recommended. It was also found that the scaling laws were independent of boundary conditions. This implies that, for a problem with complicated boundary conditions, the behavior of the prototype can be predicted from the experimental results of the corresponding scaled model given that the boundary conditions of both systems are identical. This concept is especially beneficial for problems where the boundary conditions cannot be numerically modeled in the numerical solutions but can be built in the scaled model.

In addition to a simple-supported rectangular thin plate, the similitude theory was moreover applied to the elastically restrained flat plates subjected to dynamic loads by Wu [7]. The author showed that the geometric, kinematic and dynamic similarities must be satisfied to assure the complete similitude. A similar concept was also applied to the dynamic analysis of rectangular plates under a moving load line [8]. Both complete and partial similitude cases were presented. An agreement between the theoretical vibration response of the full-scale prototype and the prediction from the solution of the scale model was obtained. Wu et al. [9] employed the similitude concept with a more complex structure where a scale model and the scaling law were utilized to determine the vibration characteristics of a full-size crane structure.

In past studies, the scaling laws were usually verified using analytical or numerical solutions. An exact agreement between the scaled solutions and theoretical solutions is always achieved for complete similitude cases. This so-called numerical experiment demonstrates that the derived scaling laws are accurate theoretically. However, its accuracy is not necessarily guaranteed when it is applied to practical engineering problems. In the present study, the scaling law for the vibration response of thin isotropic plates was therefore verified using experimental results of the model and prototype systems. The scaling law for the natural frequency of rectangular aluminum plates was derived and used to predict the natural frequency of the prototype system utilizing the experimental results of the model system. The accuracy of the scaling law was determined by comparing the scaled natural frequencies with the measured ones. The limitations of employing the scaling law for the vibration of thin plate problems are given along with some precautions in setting up the experiment on the model system.

2. Natural frequency of rectangular plates

The classical differential governing equation for the vibration of isotropic rectangular thin plates can be written as [10]

$$\frac{\partial^4 W(x,y,t)}{\partial x^4} + 2\frac{\partial^4 W(x,y,t)}{\partial x^2 \partial y^2} + \frac{\partial^4 W(x,y,t)}{\partial y^4} + \frac{\rho}{D}\frac{\partial^2 W(x,y,t)}{\partial t^2} = 0, \tag{1}$$

where W is the displacement in the out-of-plane direction, ρ is the mass density per unit area of the specimen, and D is the flexural rigidity of the plate. Assuming that the out-of-plane displacement is separable as a

function of position and time, i.e. $W(x,y,t) = w(x,y)T(t)$, the governing equation is reduced to

$$\frac{\partial^4 w}{\partial x^4} + 2\frac{\partial^4 w}{\partial x^2 \partial y^2} + \frac{\partial^4 w}{\partial y^4} - \frac{\omega^2 \rho}{D} w = 0, \tag{2}$$

where w is function of x and y only and ω is the natural frequency of the vibration.

With given boundary conditions, the vibration governing equation, Eq. (2), can be solved using either an analytical or numerical method. For simple-supported plates, the analytical closed-form solution is possible by assuming the out-of-plane displacement of the vibrated plate in the form of

$$w(x,y) = w_{mn} \sin\frac{m\pi x}{a} \sin\frac{n\pi y}{b}, \tag{3}$$

where a and b are the dimensions of plate in the x and y directions, respectively. By substituting the assumed displacement function $w(x,y)$ into the governing equation, the natural frequency of the plate is obtained and written as

$$\omega_{mn} = \frac{\pi}{2a^2}\sqrt{\frac{D}{\rho}}\left(m^2 + \frac{a^2}{b^2}n^2\right), \tag{4}$$

where ω_{mn} are the natural frequencies of the plate in Hz, m and n are positive integers. It should be noted that, for plates with other boundary conditions, the natural frequencies are not available in the form of exact analytical expression. The numerical or finite element methods are required for specimens with clamped or free boundary conditions.

3. Scaling law for the vibration of plate

Although the natural frequencies of thin plates with combinations of simple support, clamped support or free boundary conditions are available, they may not be practically appropriate for engineering structures where accurate natural frequencies are required. The boundary conditions of practical structures are usually non-classical ones such as elastically restrained or imperfect boundary conditions, which are not easily modeled because the level of restraining is unknown. This is where the scaling law can be utilized to determine the vibration behavior of the structure or prototype of interest using the experimental results of the scaled model. The scaled model is either a scaled-down or scaled-up test specimen having complete similarity with the real structure. Although the boundary conditions of the prototype are not exactly known, they can be modeled in the scaled model using similar supports. Thus, the experimental results from the corresponding test specimen along with the scaling law can be used to predict the vibration behavior of the prototype. The derivation of the scaling law for vibration behavior is briefly derived in this section.

The scaling law for the vibration of rectangular isotropic plates is derived from the governing equation, Eq. (2), by comparing the governing equations of the model with that of the prototype. From both equations, the similitude invariant term, which leads to the scaling law, is obtained. Let the variables of the prototype and their corresponding model variables be related to each other as follows:

$$x_p = C_x x_m, \quad y_p = C_y y_m, \quad w_p = C_w w_m, \quad D_p = C_D D_m,$$
$$\omega_p = C_\omega \omega_m, \text{ and } \rho_p = C_\rho \rho_m,$$

where subscripted p refers to the prototype system and subscripted m refers to the model system, and C_i are the scaling factors of the i parameters. To derive the similitude invariant, the governing equations of the model and prototype are written as the following:

$$\frac{\partial^4 w_m}{\partial x_m^4} + 2\frac{\partial^4 w_m}{\partial x_m^2 \partial y_m^2} + \frac{\partial^4 w_m}{\partial y_m^4} - \frac{\omega_m^2 \rho_m}{D_m} w_m = 0, \tag{5}$$

$$\frac{C_w}{C_x^4}\frac{\partial^4 w_m}{\partial x_m^4} + 2\frac{C_w}{C_x^2 C_y^2}\frac{\partial^4 w_m}{\partial x_m^2 \partial y_m^2} + \frac{C_w}{C_y^4}\frac{\partial^4 w_m}{\partial y_m^4} - \frac{C_\omega^2 C_\rho C_w}{C_D}\frac{\omega_m^2 \rho_m}{D_m} w_m = 0. \tag{6}$$

It should be noted that Eq. (6) can be written in the same form as Eq. (5) with subscript "p" instead of subscript "m." However, the scaling factors are utilized so that the governing equations of both systems can be compared and simplified. Comparing both equations, the vibration behavior of the model and of the prototype are similar if groups of the scaling factors in Eq. (6) are all equal. This implies that Eq. (6) can be reduced to Eq. (5) when the scaling factor groups are canceled out. Thus, the similitude requirement is obtained as

$$\frac{1}{C_x^4} = \frac{1}{C_x^2 C_y^2} = \frac{1}{C_y^4} = \frac{C_\omega^2 C_\rho}{C_D}. \tag{7}$$

By assuming that the model and prototype have a geometric similarity ($C_x = C_y = C_a = C_b$), the similarity requirement is simplified to

$$\frac{C_\omega^2 C_\rho C_b^4}{C_D} = 1. \tag{8}$$

Eq. (8) is the similitude invariant of the vibration behavior of rectangular plates. This invariant can be reduced to the scaling law of plate natural frequency as

$$\omega_p^2 = \omega_m^2 C_D \frac{b_m^4 \rho_m}{b_p^4 \rho_p}. \tag{9}$$

This scaling law relates the natural frequencies of the model to that of the corresponding prototype. The derived scaling law is valid for a model–prototype pair with complete geometric similarity, i.e. $C_a = C_b$ or both systems having the same aspect ratio. The scaling law can be verified with the theoretical solution shown in the previous section. As shown in Table 1, rectangular aluminum plates with $b = 250$ mm and an aspect ratio, a/b, of 1–3.5 are selected as models and used to predict the natural frequencies of the stainless steel prototypes with a width b of 200 and 300 mm, respectively. The model plates are assumed to be Al6061-T6 with $E = 68.9$ GPa, $v = 0.35$, density $= 2.71 \times 10^3$ kg/m^3, and plate thickness $h = 2$ mm, while the prototypes are stainless steel with $E = 193$ GPa, $v = 0.27$, density $= 7.86 \times 10^3$ kg/m^3, and plate thickness $h = 2$ mm. The fundamental natural frequencies of the models determined from the analytical solution, Eq. (4), are shown in column 2. These natural frequencies are substituted into the scaling law to predict the scaling natural frequencies of the prototypes, as presented in the "ω_{Scaling}" columns. The scaling frequencies are verified by the theoretical solutions shown in column 3 and 5. The data confirms that the natural frequencies determined from the scaling law and those from the closed-form solutions are identical.

Therefore, the scaling law for the natural frequency of rectangular plate is verified, theoretically. The derived scaling law is applicable to a model and prototype pair with the same aspect ratio, although they are made of different materials. However, it is not assured that the scaling law will be accurate in real applications. The objective of the present study was therefore to validate the scaling law with the experiment results. Thus, vibration experiment was performed to determine the natural frequencies of the model and prototype

Table 1
The fundamental natural frequencies in Hz for Al6061-T6 specimens

Aspect ratio (a/b)	Aluminum model $b = 250$ mm	Stainless steel prototype			
		$b = 200$ mm		$b = 300$ mm	
		ω_{Theory}	ω_{Scaling}	ω_{Theory}	ω_{Scaling}
1.0	156.2	233.4	233.3	103.7	103.7
1.5	112.8	168.5	168.5	74.9	74.9
2.0	97.6	145.9	145.8	64.8	64.8
2.5	90.6	135.4	135.4	60.2	60.2
3.0	86.8	129.6	129.6	57.6	57.6
3.5	84.5	126.2	126.2	56.1	56.1

specimens. The measured natural frequencies of the models were then substituted into the scaling law to predict the natural frequencies of the prototypes. Subsequently, the scaling frequencies of the prototype were compared with the measured ones to determine the accuracy of the derived scaling law.

4. Experimental setup

Several samples of thin rectangular plates were tested to determine their first three natural frequencies. The specimens were composed of aluminum, structural steel and stainless steel rectangular thin plates. The boundary conditions of the test panels were a combination of the knife-edge support and free boundary conditions. The knife-edge support was employed to simulate the theoretically simple-supported boundary condition. Schematic drawings of the specimens' dimensions and boundary conditions are shown in Fig. 1. The boundary of specimen supported by the knife-edge constraint is designated as "S," while the free supported edge is represented by "F." The boundary conditions of the specimens used in this study were SSSS, SFSS, SFSF, and SSFF, as shown in the figure. The first and second letters represent the boundary condition on the $y = 0$ and b edges, respectively. Similarly, the last two letters symbolize the boundary conditions on the other edges. The specimens were mounted in the test setup and equipped with an impact hammer and an accelerometer as shown in Fig. 2. The knife-edge support replicating the simply supported boundary condition was enforced by two stainless steel bars coupled on the specimen. The steel bars were machined in an inclined direction to form a knife-edge. With this support, the specimens were intentionally allowed to freely rotate but any out-of-plane displacement was restrained. The knife-edge supports were fixed with steel boxes with a number of machine screws. Additional machine screws were also used to push the knife-edge supports against the specimen surface. The assembly of steel boxes and knife-edge supports was also tested for natural frequency to confirm that their natural frequencies were not in the range of those of the specimens.

The vibration test for natural frequency was performed using an impact test [11,12]. Briefly, the specimens were excited by an impact hammer while the applied impulse was monitored by a dynamic signal analyzer. An accelerometer was placed on the specimen at a selected location to measure the plate response in terms of acceleration. It is recommended that the accelerometer should not be set on the node line of the vibration to avoid a low response signal. If the node line is unknown or uncertain, more than one measurement is recommended. In the present study, several pretests were conducted to determine a suitable location of the accelerometer. Besides the applied impulse from the impact hammer, the acceleration responses from the accelerometer were collected by a dynamic signal analyzer. The accelerations were recorded five times from five excitations of the impact hammer. These five sets of the acceleration data measured in the time domain were processed by a fast Fourier transform (FFT) algorithm using the dynamic signal analyzer to obtain the response in the frequency domain. From the vibration response in the frequency domain, the natural

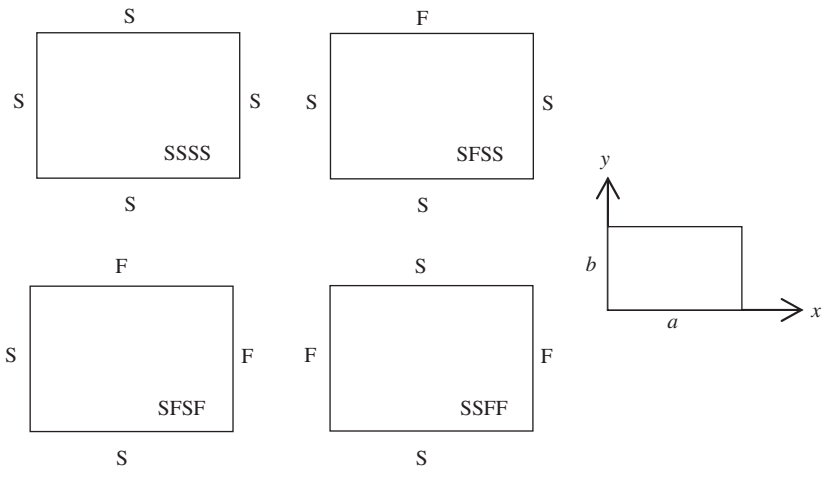

Fig. 1. Schematic drawings of the rectangular test specimens.

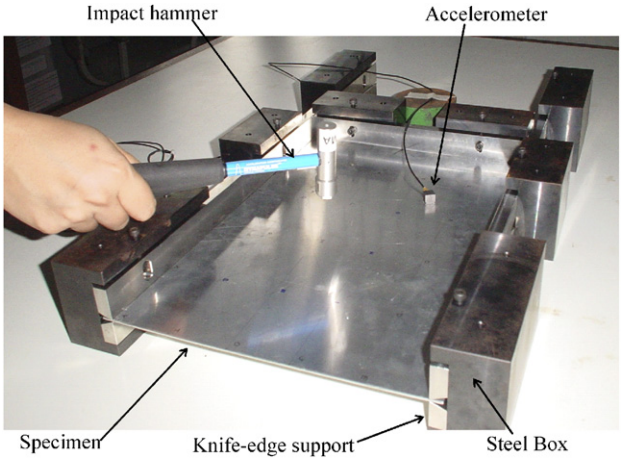

Fig. 2. Experimental setup with accelerometer and impact hammer.

frequencies of the specimen were identified from the peak of the response. Theoretically, there are infinite numbers of natural frequency; however, only the first three modes are of interest in this study. Fig. 3 shows examples of the vibration response measured in the frequency domain obtained from the dynamic signal analyzer for a $300 \times 300\,\mathrm{mm}^2$ aluminum plate with various boundary conditions. The measured natural frequencies in Hz for the first three modes of the specimen with SSSS boundary conditions are 149.0, 293.5, and 322.5 Hz, respectively. A response similar to those of shown in Fig. 3 can be obtained from experiments with excitation and accelerometer located at various positions. Ideally, the measured natural frequencies are independent of the location of either excitation or accelerometer. From the experiments, varying the position of excitation and the location of the response measurement has a minimal effect on the measured natural frequencies. In this study, a minimum of 5 experiments were performed for each specimen and the experimental natural frequency was determined from the average of each measurement.

5. Experimental results

Two sets of the experiment were conducted in this study to determine the accuracy of the scaling law using experimental measurements in two cases, i.e. (a) aluminum model and prototype of different sizes and (b) equal-size model–prototype pairs composed of different materials. The former part of the study was designed to investigate the size effect, while the material effect was studied in the latter part. To examine the size effect, the test specimens were nine aluminum plates with aspect ratios (a/b) of 1, 1.5, and 2 and a specimen nominal width b of 200, 250, and 300 mm, respectively. The natural frequencies of all the specimens with four combinations of boundary conditions were experimentally determined and used to validate the scaling law. The other set of experiments involved tests on four groups of specimens, i.e. two groups of aluminum, a group of structural steel and a group of stainless steel. The dimensions of the specimens in this set of experiments were $300 \times 200\,\mathrm{mm}^2$ and $375 \times 250\,\mathrm{mm}^2$.

5.1. Size effect

For the first part of the experiment, the measured natural frequencies for the SSSS aluminum plates with nine different dimensions are presented in Table 2. In the table, the test specimens are classified into three groups: rectangular plates with aspect ratios of 1, 1.5, and 2. The experimental data showed that the natural frequencies decreased with plate size. Similar experimental results were obtained for aluminum specimens with other boundary conditions but are not presented here. The specimens shown in Table 2 were assumed to be a model or a prototype and used to validate the scaling law, as shown in Table 3. From the three specimens with an aspect ratio of 1, three pairs of models and prototypes were assigned to the test specimens. As shown in

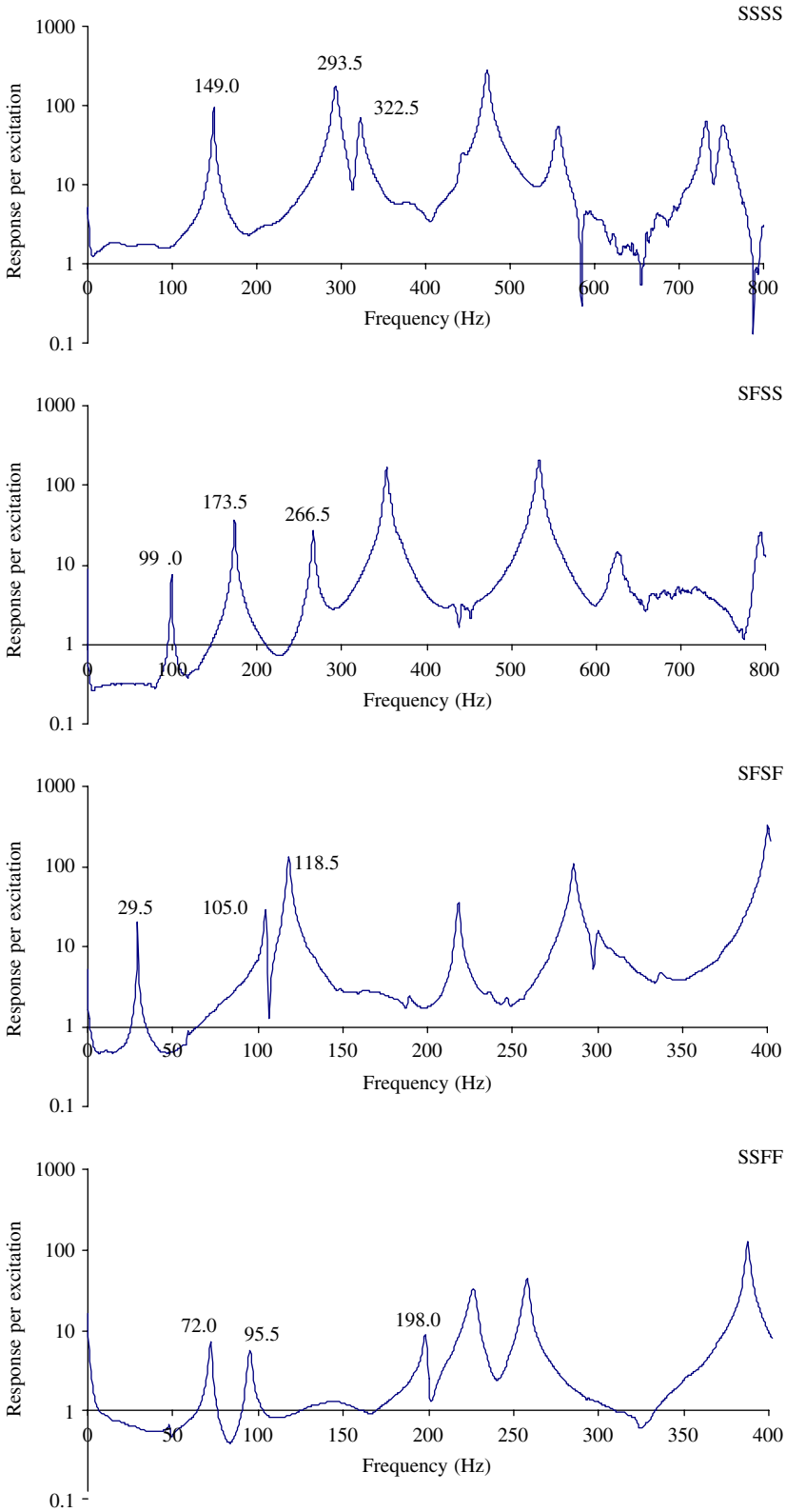

Fig. 3. Vibration response in frequency domain of $300 \times 300\,\text{mm}^2$ aluminum plate.

Table 2
Measured natural frequencies of the SSSS aluminum specimens

Aspect ratio	Specimen size, $a \times b$ (mm^2)	Natural frequency (Hz)		
		1st mode	2nd mode	3rd mode
1	200×200	309.8	676.9	729.6
	250×250	196.7	409.0	444.6
	300×300	148.8	293.2	321.8
1.5	300×200	221.2	376.3	580.7
	375×250	150.5	255.4	376.6
	450×300	99.6	171.4	257.4
2	400×200	199.6	256.2	425.2
	500×250	132.4	173.6	275.5
	600×300	90.1	117.8	193.4

Table 3
The measured and scaling natural frequencies for the SSSS aluminum specimens

Aspect ratio	Model	Prototype	Mode	Model	Prototype		
					ω_{Exp}	$\omega_{Scaling}$	%Dis
1	200×200	300×300	1	309.8	148.8	137.7	−7.47
			2	676.9	293.2	300.8	2.61
			3	729.6	321.8	324.3	0.77
	250×250	200×200	1	196.7	309.8	307.3	−0.79
			2	409.0	676.9	639.1	−5.59
			3	444.6	729.6	694.7	−4.79
	300×300	250×250	1	148.8	196.7	214.3	8.93
			2	293.2	409.0	422.2	3.23
			3	321.8	444.6	463.4	4.23
1.5	300×200	450×300	1	221.2	99.6	98.3	−1.29
			2	376.3	171.4	167.2	−2.42
			3	580.7	257.4	258.1	0.27
	375×250	300×200	1	150.5	221.2	235.2	6.31
			2	255.4	376.3	399.1	6.05
			3	376.6	580.7	588.4	1.33
	450×300	375×250	1	99.6	150.5	143.4	−4.70
			2	171.4	255.4	246.8	−3.36
			3	257.4	376.6	370.7	−1.58
2	400×200	600×300	1	199.6	90.1	88.7	−1.54
			2	256.2	117.8	113.9	−3.34
			3	425.2	193.4	189.0	−2.29
	500×250	400×200	1	132.4	199.6	206.9	3.64
			2	173.6	256.2	271.3	5.87
			3	275.5	425.2	430.5	1.24
	600×300	500×250	1	90.1	132.4	129.7	−2.01
			2	117.8	173.6	169.6	−2.29
			3	193.4	275.5	278.5	1.09

column 2 and 3 of Table 3, a $200 \times 200\,mm^2$ specimen was set as a model and used to model the $300 \times 300\,mm^2$ prototype specimen. The other two model–prototype pairs were a $250 \times 250\,mm^2$ model with $200 \times 200\,mm^2$ prototype and a $300 \times 300\,mm^2$ model with $250 \times 250\,mm^2$ prototype. Specimens with aspect ratios of 1.5 and 2 were also assigned as models or prototypes in the same approach. In Table 3, columns 5 and 6 are the

measured natural frequencies of the model and prototype, respectively. The next column labeled as "ω_{Scaling}" presents the scaling natural frequencies of the prototypes. These scaling natural frequencies were determined from the scaling law shown in Eq. (9) using the measured natural frequencies of the model in column 5. The experimental and scaling natural frequencies shown in columns 6 and 7, respectively, were compared with each other. The percentage discrepancy of the scaling natural frequency shown in the last column was determined according to

$$\%\text{Dis} = \frac{\omega_{\text{Scaling}} - \omega_{\text{Exp}}}{\omega_{\text{Exp}}} \times 100\%. \tag{10}$$

Most of the comparisons show a good agreement between the scaling and measured natural frequency. The average of the absolute values of percentage discrepancy for experiment on all 27 model–prototype pairs is 3.30% with a standard deviation of 4.05%. The minimum and maximum percentage discrepancies are −7.47% and +8.93%, respectively, while more than half of the comparisons have a percentage discrepancy within ±3%. There was no significant difference in percentage discrepancy for each vibration mode or plate aspect ratio. The causes of discrepancy between the scaling and measured natural frequencies are probably related to the imperfections of the boundary conditions and specimens. As described in the previous section, knife-edge supports of the test setup were controlled by several machine screws. In the experiments, the machine screws were tightened until the gaps between the specimen and support were invisible. Although it was desired to obtain identical boundary conditions for the model and its prototype, it was expected that the boundary conditions for each experiment would not be perfectly identical. Besides the imperfect boundary conditions, imperfections of specimens such as non-uniform thickness and the existence of plate curvature might be the cause of discrepancy between the scaling and measured behaviors. These two causes of error are classified as an experimental uncertainty, which is typical in experimental study and is very difficult to completely eliminate.

Another three comparable studies were performed on the same test specimens with boundary conditions of SFSS, SFSF, and SSFF. An inconsistency between the scaling and measured natural frequencies of all comparisons in terms of percentage discrepancy is shown in Table 4. The last two rows of the table show the average of absolute values of percentage discrepancy and the standard deviation of the percentage discrepancy, respectively. The overall average and standard deviations of the percentage discrepancy were 4.90% and 6.46%, respectively. The histogram in Fig. 4 represents the frequency distribution of the percentage discrepancy, which revealed that the distribution of the percentage discrepancy closely resembles a normal distribution and the percentage discrepancies of 95 from 108 comparisons were in the range of ±10%. However, percentage errors for some pairs of model and prototype were slightly higher, especially for the experiments on the SFSF specimens. Eight values of percentage discrepancy from the experiments on this

Table 4
Percentage discrepancy between scaling and measured natural frequencies

Aspect ratio	Model	Prototype	SSSS			SFSS			SFSF			SSFF		
			Mode1	Mode2	Mode3	Mode1	Mode2	Mode3	Mode1	Mode2	Mode3	Mode1	Mode2	Mode3
1	200 × 200	300 × 300	−7.47	2.61	0.77	−0.86	3.75	0.06	−5.56	−2.12	−4.52	3.55	2.80	2.05
	250 × 250	200 × 200	−0.79	−5.59	−4.79	2.91	−2.62	2.19	1.37	0.45	−0.58	0.89	−4.90	−0.19
	300 × 300	250 × 250	8.93	3.23	4.23	−1.98	−1.03	−2.20	4.46	1.72	5.35	−4.28	2.30	−1.83
1.5	300 × 200	450 × 300	−1.29	−2.42	0.27	7.26	2.83	6.84	−17.74	−10.07	−10.96	−9.00	−15.54	−0.86
	375 × 250	300 × 200	6.31	6.05	1.33	−11.91	−8.50	−5.50	13.41	6.00	5.41	7.06	5.42	3.15
	450 × 300	375 × 250	−4.70	−3.36	−1.58	5.84	6.28	−0.95	7.19	4.90	6.54	2.64	12.31	−2.21
2	400 × 200	600 × 300	−1.54	−3.34	−2.29	3.94	2.75	2.57	−11.22	−14.29	−9.69	−6.24	−12.66	−6.07
	500 × 250	400 × 200	3.64	5.87	1.24	2.06	1.00	−0.46	−6.78	−1.55	2.48	−3.51	8.36	5.92
	600 × 300	500 × 250	−2.01	−2.29	1.09	−5.73	−3.64	−2.06	20.84	18.51	8.06	10.54	5.67	0.52
Average				3.30			3.62			7.47			5.20	
Standard deviation				4.05			4.63			9.46			6.64	

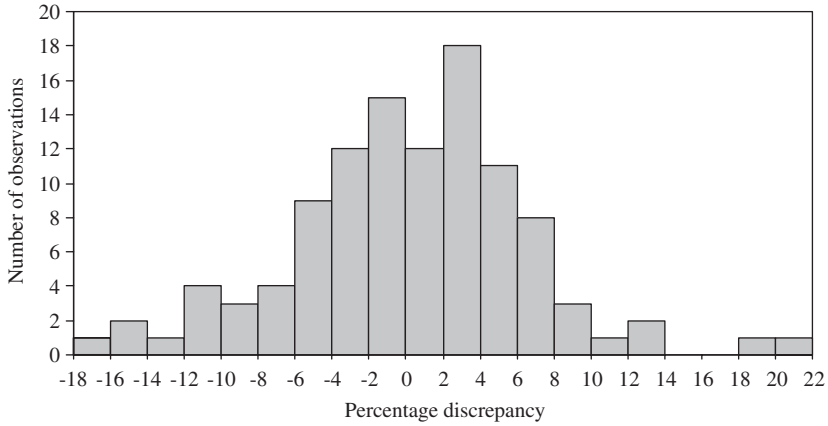

Fig. 4. Histogram of the percentage discrepancy between scaling and measured natural frequencies.

boundary condition resulted in a percentage discrepancy higher than $\pm 10\%$, compared with only four values and one value for SSFF and SFSS cases, respectively. The average of the absolute percentage discrepancy for SFSF specimens was 7.47%, which is higher than those of other boundary conditions. The higher percentage discrepancy of the scaling law observed in specimens with SFSF boundary conditions was probably caused by the particular characteristics of these boundary conditions. For SFSF specimens, the free boundary condition was imposed on two adjacent edges of the plate, i.e. two adjacent edges were free to move, as shown in Fig. 1. As a result, the specimen with this combination of boundary conditions tended to be slightly curved at the free corner because of its own weight. The degree of non-flatness of the test specimens was probably different for specimens with different dimensions, that is, the size effect had an influence on the accuracy of the scaling law in this case. So, the model and prototype with these boundary conditions did not have a complete similarity, resulting in a slightly higher percentage discrepancy for these specific boundary conditions.

Therefore, from the experimental study in the first part, the scaling law provided reasonable accuracy for modeling a prototype using a model with different dimensions. Uncertainties of the experiments in boundary condition and thickness are believed to be the sources of the discrepancy. To obtain a decent prediction from the scaling law, the experiment on the model specimen should be carefully performed to assure near-complete, if not perfectly complete, similarity with the prototype. The specimen size might slightly affect the precision of the scaling law in case of SFSF specimens because the flatness of the model and prototype cannot be maintained.

5.2. Material effect

The second part of the study was to determine the applicability of using a model with one type of material to predict the vibration behavior of the prototype made from another type of material. Four types of specimen including two types of aluminum specimen; called herein Aluminum-A and Aluminum-B, and the other two groups of steel and stainless steel specimens were tested. All specimens are commercially available in form of sheet metal. They were prepared and machined to the nominal dimensions of $300 \times 200\,\mathrm{mm}^2$ and $375 \times 250\,\mathrm{mm}^2$. The physical and mechanical properties of all the materials were experimentally determined and are presented in Table 5. It should be noted that the mechanical properties of Aluminum-A and Aluminum-B are more or less comparable and so are the properties of steel and stainless steel. Therefore, a total of eight thin plates were tested in this part of the study. Since material effect was investigated in this study, only specimens of the same size were assigned as a model–prototype pair. All specimens with four different boundary conditions were tested for the first three natural frequencies. The test results were then assigned as experimental natural frequencies of the model or the prototype. The accuracy of the scaling law was determined by comparing the scaling and experimental natural frequencies in the same manner as the previous study. Lists of the percentage discrepancies between both natural frequencies are shown in Table 6.

Table 5
Properties of materials used in the second part of the experiments

Material	Thickness (mm)	Mass density per area (kg/m^2)	Modulus of elasticity (GPa)	Poisson ratio
Aluminum-A	1.81	5.10	62.3	0.316
Aluminum-B	1.42	3.63	58.0	0.320
Steel	1.95	15.29	197.0	0.346
Stainless steel	1.48	11.23	200.0	0.327

Table 6
Percentage discrepancies between scaling and measured natural frequencies demonstrating the material effect

Model	Prototype	Specimen size, $a \times b$ (mm^2)	SSSS			SFSS			SFSF			SSFF			Avg.
			Mode1	Mode2	Mode3	Mode1	Mode2	Mode3	Mode1	Mode2	Mode3	Mode1	Mode2	Mode3	
Al-A	Al-B	300 × 200	−11.61	−4.67	−5.15	14.40	6.51	6.67	−11.72	6.12	−1.85	4.55	1.51	5.36	6.68
		375 × 250	−12.39	−1.71	−3.65	3.74	−4.28	−2.67	−8.44	−7.61	5.06	0.62	2.82	-1.77	4.56
	Steel	300 × 200	19.58	16.51	19.94	36.13	23.16	25.86	12.02	7.30	12.12	24.56	14.97	19.69	19.32
		375 × 250	26.84	27.68	18.63	21.57	14.04	18.60	19.94	7.45	16.24	33.47	20.87	23.96	20.77
	Stainless steel	300 × 200	22.11	23.80	22.48	34.08	27.18	29.63	12.37	11.87	19.42	33.50	22.67	29.91	24.09
		375 × 250	27.03	32.71	24.02	23.71	20.23	22.16	17.06	13.24	24.82	34.32	28.02	21.06	24.03
Al-B	Steel	300 × 200	35.29	22.22	26.45	18.99	15.63	17.99	26.89	1.12	14.23	19.14	13.26	13.61	18.74
		375 × 250	44.77	29.90	23.13	17.19	19.14	21.85	30.99	16.30	10.64	32.65	17.55	26.20	24.19
	Stainless steel	300 × 200	38.15	29.87	29.13	17.20	19.41	21.52	27.28	5.42	21.67	27.69	20.84	23.30	23.46
		375 × 250	44.99	35.01	28.72	19.25	25.61	25.51	27.85	22.56	18.81	33.49	24.51	23.24	27.46
Steel	Stainless steel	300 × 200	2.11	6.26	2.12	−1.51	3.26	2.99	0.31	4.26	6.51	7.18	6.69	8.53	4.31
		375 × 250	0.15	3.94	4.54	1.76	5.43	3.00	−2.40	5.39	7.38	0.64	5.92	−2.34	3.57

The first two columns of the table are materials of the model and prototype, respectively, with the specimen dimensions shown in column 3. The next twelve columns indicate the percentage discrepancies between the scaling and measured natural frequencies. The last column shows the averages of absolute percentage discrepancy for each pair of model and prototype. Clearly, the degree of discrepancy was separated into two groups; the lower one and the higher one. The scaling natural frequencies were well correlated with the measured ones for model–prototype pairs with the same type of material, i.e. a pair of Aluminum-A and Aluminum-B or a pair of steel and stainless steel. The averages of absolute percentage discrepancy for these model–prototype pairs were in the range of 3.57–6.68%. On the contrary, the scaling natural frequencies did not match the corresponding experimental results well for a pair of model and prototype with different types of material, for example, the Aluminum-A model and steel prototype or the Aluminum-B model and stainless steel prototype. The average percentage discrepancies varied from 18.74% to 27.46%. These fairly high percentage discrepancies are contradictory to the theoretical validation of the scaling law, shown in Table 1. It is proved that the scaling law is theoretically precise although both model and prototype are composed of different materials. These high percentage discrepancies can be explained by considering the boundary conditions provided by the experimental setup. Although aluminum or steel plates were restrained by the same knife-edge supports, they were probably not subjected to similar boundary conditions because of the difference between the stiffness of the knife-edge supports and the stiffness of the test specimens. The knife-edge supports which were used to simulate the simply supported boundary condition were made of stainless steel with an elastic modulus of about 200 GPa. Because of the comparable stiffness, when steel or stainless steel specimens were mounted on the knife-edge support, an approximate simple support was achieved, supposedly. On the other hand, it would seem that a near-clamped support was obtained for the experiments of the aluminum plates due to the mismatch in stiffness between the specimen and the support. This hypothesis

can be tested by comparing the experimental results of the SSSS specimens with the theoretical solutions, as shown in Fig. 5. The experimental natural frequencies of all eight specimens with knife-edge supports on all edges, i.e. SSSS specimens, were plotted and compared with the theoretical solutions. In the figure, the experimental natural frequencies of the first three vibration modes of both $300 \times 200\,\mathrm{mm}^2$ and $375 \times 250\,\mathrm{mm}^2$ specimens with different materials are shown, labeled as "Exp". The theoretical natural frequencies of the specimens with all edges simple supported and all edges clamped were also plotted, labeled as "Theory (SSSS)" and "Theory (CCCC)," respectively. Obviously, all of the experimental natural frequencies of the aluminum specimens (both Aluminum-A and Aluminum-B) were close to the theoretical solutions of the CCCC specimens. In contrast, the experimental results of the steel and stainless steel specimens closely approximated to the theoretical solutions of the SSSS specimens. Because of the greater stiffness of the support, the aluminum specimens were probably not allowed to rotate as much as the steel specimens were, although they were constrained by the same supports. Therefore, the boundary condition provided by the experimental setup, which was supposed to be simple support, was a fairly clamped boundary condition for the aluminum specimens. For the steel specimens, the near simply supported boundary condition was successfully obtained as intended. That is, the very same knife-edge support provided quite different boundary conditions for the aluminum and steel specimens because the kinetic conditions of both types of material were different. The high percentage discrepancy in this case was not caused by experimental uncertainty as of those in Section 5.1, but was the result of the dissimilar boundary conditions which violated the similarity requirements. It is concluded that, in practice, the type of material of the model indirectly affects the accuracy of the scaling law because specimens with different types of material may be supported differently by the same support.

To confirm that the derived scaling law is applicable for a model and prototype composed of different materials if their boundary conditions are sufficiently comparable, an additional set of experiments was performed. The supplementary tests were similar to the experiments shown in Table 6 but boundary conditions for the specimens were free boundary condition on all edges (FFFF). The specimens used in the experiment included all four groups of materials with plate dimensions of $300 \times 200\,\mathrm{mm}^2$ and $375 \times 250\,\mathrm{mm}^2$. The FFFF boundary condition was set up by hanging the test specimen using a small rope. With this test setup, the specimens were allowed to freely vibrate in an out-of-plane direction when excited by the impact hammer. The first three natural frequencies were experimentally determined and assigned as a model or a prototype similar to the study shown in Table 6. The percentage discrepancies between the scaling and measuring natural frequencies for the experiment with FFFF boundary conditions are presented in Table 7.

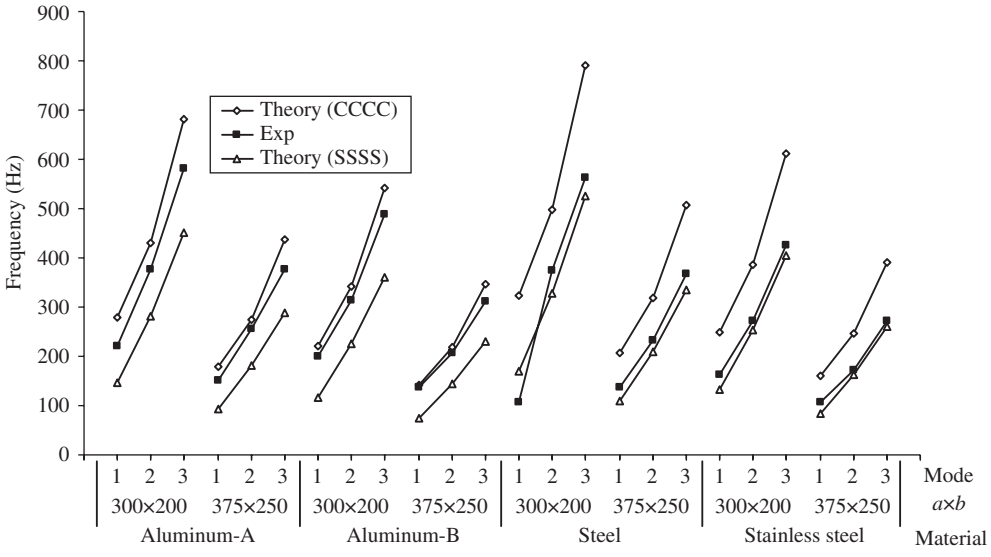

Fig. 5. Experimental and theoretical natural frequencies of the SSSS specimens.

Table 7
Percentage discrepancies between scaling and measured natural frequencies of FFFF specimens

Model	Prototype	Specimen size, $a \times b$ (mm^2)	FFFF			Avg.
			Mode1	Mode2	Mode3	
Al-A	Al-B	300×200	10.47	−2.39	9.59	7.48
		375×250	14.15	3.53	7.11	8.26
	Steel	300×200	2.86	9.71	4.06	5.54
		375×250	5.71	−3.17	−7.84	5.57
	Stainless steel	300×200	2.28	6.98	9.13	6.13
		375×250	14.66	1.15	−1.53	5.78
Al-B	Steel	300×200	−6.89	12.39	−5.05	8.11
		375×250	−7.40	−6.47	−13.95	9.27
	Stainless steel	300×200	−7.42	9.59	−0.42	5.81
		375×250	0.45	−2.30	−8.06	3.60
Steel	Stainless steel	300×200	−0.57	−2.49	4.87	2.64
		375×250	8.47	4.46	6.84	6.59

The scaling law was able to predict the natural frequency of the prototype fairly well. From 36 comparisons, only 5 model–prototype pairs had a percentage error higher than $\pm 10\%$. The averages of absolute percentage discrepancy for each pair of model and prototype ranged from 2.64% to 9.27%. Unlike the experiments shown in Table 6, there is no significant difference in percentage error between specimens of the same and different types of materials. Experimental results from either aluminum or steel models were able to predict the behavior of the prototypes with comparable accuracy. A good prediction by scaling law is achieved in the experiment with FFFF boundary conditions because of the similarity of the boundary conditions of the model and prototype. Without a support, it is assured that the boundary conditions of the model and prototype are similar, geometrically and kinetically. Thus, the scaling law is applicable for a model and prototype composed of different materials if the boundary conditions of both systems have sufficient similarity. The boundary conditions of two systems are said to be identical if they have geometric and kinetic similarities. The same set of supports may not provide identical boundary conditions for each specimen because of the mismatch of material properties between specimen and support causing kinetic dissimilarity.

6. Conclusions

This study derives the scaling law and similitude requirements for vibration response of rectangular thin plates. The scaling law was theoretically verified and found to be exact for a pair of models and prototypes with complete similarities. To determine the accuracy of the scaling law in practice, an experimental setup was prepared to accommodate the vibration experiment. The specimen was excited by an impact hammer and measured for vibration response using an accelerometer. The natural frequencies could be identified from the peaks of the response in the frequency domain. In the first part of the experiment, the scaling law was applied to a pair of models and prototypes with the same material. From 108 comparisons, the average percentage error between the scaling and experimental natural frequencies was 4.90%. This fairly low percentage discrepancy confirms that scaling law is accurate and practical in engineering applications. The experimental uncertainty in term of imperfect boundary conditions and specimens is probably the cause of this slight discrepancy. However, it is noticed that the scaling natural frequency for some cases of SFSF plates did not correspond well with the measured data. The sources of this error were not only caused by the experiment uncertainty but also caused by the fairly high degree of dissimilarity between the model and prototype specimens, i.e. curvature of the test specimens due to two adjacent edges having no support. For specimens with a combination of these particular boundary conditions, the size effect influenced the accuracy of the scaling law because of the dissimilarity in plate configuration of the model and prototype. In the second part of the study, natural frequencies of the prototypes were predicted using model specimens of different

materials. The data shows that the scaling natural frequencies were not very well matched to the experimental ones if the model and prototype were composed of different types of materials. In comparison with the theoretical solutions, it is believed that the boundary conditions of the model and prototype are different, resulting in a very high percentage discrepancy of the scaling natural frequency. This suggests that boundary conditions on the test specimens are not only dependent on the geometry of the support but also on the kinetic conditions of the support. Additional experiments were performed on specimens made of different materials using FFFF boundary condition to validate the scaling law for model and prototype with identical boundary conditions and composed of different materials. Without a support, the boundary conditions of the model and prototype are identical, thus, the accuracy of the scaling law is achieved as expected.

In conclusion, the derived scaling law is practical to employ in engineering applications. From this study, the discrepancy of the scaling solutions might develop from the uncertainty of the experiment, curvature of the specimens due to two adjacent free edges, and dissimilar boundary conditions due to a mismatch in the material properties of the specimen and support. Errors from the uncertainty of the experiment are fewer than those from other sources and can be kept minimal by carefully setting up the experimental conditions on the model to match those of the prototype. This type of error is typical in the experimental investigation and impossible to completely eliminate in practice. Errors from the latter two sources, on the other hand, are the result of the incomplete similarity conditions between the model and prototype. These causes of error could be eliminated by ensuring that the plate configurations and boundary conditions of both systems are completely identical. To utilize the scaling law, precautions should be taken for a specimen with some particular combinations of boundary conditions where plate configurations might be effected by the size of the test specimen. Moreover, without a procedure to obtain a complete similarity of boundary conditions of the model and prototype with different materials, it is strongly recommended that the model is prepared from the same material as the prototype. It is also worthwhile to further study the possibility of overcoming the difficulties in utilizing the support on different materials as well as the chance of deriving a scaling law for a model–prototype pair with different boundary conditions.

Acknowledgments

This research is supported by the Commission on Higher Education and Thailand Research Fund under project Grant No. RMU4880021.

References

[1] E. Szucs, *Similitude and Modelling*, Elsevier Scientific Publishing Co., New York, 1980.
[2] G.J. Simitses, Structural similitude for flat laminated surfaces, *Composite Structures* 51 (2001) 191–194.
[3] J. Rezaeepazhand, G.J. Simitses, J.H. Starnes Jr., Use of scaled-down models for predicting vibration response of laminated plates, *Composite Structures* 30 (1995) 419–426.
[4] P. Singhatanadgid, V. Ungbhakorn, Buckling similitude invariants of symmetrically laminated plates subjected to biaxial loading, *SEM Annual Conference and Exposition*, Milwaukee, WI, USA, June, 2002.
[5] P. Singhatanadgid, V. Ungbhakorn, Scaling laws for vibration response of anti-symmetrically laminated plates, *Structural Engineering and Mechanics* 14 (2002) 345–364.
[6] V. Ungbhakorn, P. Singhatanadgid, Similitude invariants and scaling laws for buckling experiments on anti-symmetrically laminated plates subjected to biaxial loading, *Composite Structures* 59 (2003) 455–465.
[7] J.J. Wu (Ed.), Letter to the editor: the complete-similitude scale models for predicting the vibration characteristics of the elastically restrained flat plates subjected to dynamic loads, *Journal of Sound and Vibration* 268 (2003) 1041–1053.
[8] J.J. Wu, Dynamic analysis of a rectangular plate under a moving line load using scale beams and scaling laws, *Computers and Structures* 83 (2005) 1646–1658.
[9] J.J. Wu, M.P. Cartmell, A.R. Whittaker, Prediction of the vibration characteristics of a full-size structure from those of a scale model, *Computers and Structures* 80 (2002) 1461–1472.
[10] D.J. Gorman, *Free Vibration Analysis of Rectangular Plates*, Elsevier, New York, 1982.
[11] J.P. Lecointea, R. Romarya, J.F. Brudnya, T. Czaplab, Five methods of stator natural frequency determination: case of induction and switched reluctance machines, *Mechanical Systems and Signal Processing* 18 (2004) 1133–1159.
[12] G.P. Zou, M. Naghipour, F. Taheri, A nondestructive method for evaluating natural frequency of glued-laminated beams reinforced with GRP, *Nondestructive Testing and Evaluation* 19 (2003) 53–65.